Rabi-Kondo correlated state in a laser-driven quantum dot

B. Sbierski,[1] M. Hanl,[2] A. Weichselbaum,[2] H. E. Türeci,[1,3] M. Goldstein,[4] L. I. Glazman,[4] J. von Delft,[2] and A. İmamoğlu[1]

[1] *Institute for Quantum Electronics, ETH Zürich, CH-8093 Zürich, Switzerland*
[2] *Arnold Sommerfeld Center for Theoretical Physics, Ludwig-Maximilians-Universität München, D-80333 München, Germany*
[3] *Department of Electrical Engineering, Princeton University, New Jersey 08544, USA*
[4] *Department of Physics, Yale University, 217 Prospect Street, New Haven, Connecticut, 06520, USA*

Spin exchange between a single-electron charged quantum dot and itinerant electrons leads to an emergence of Kondo correlations. When the quantum dot is driven resonantly by weak laser light, the resulting emission spectrum allows for a direct probe of these correlations. In the opposite limit of vanishing exchange interaction and strong laser drive, the quantum dot exhibits coherent oscillations between the single-spin and optically excited states. Here, we show that the interplay between strong exchange and non-perturbative laser coupling leads to the formation of a new non-equilibrium quantum-correlated state, characterized by the emergence of a laser-induced secondary spin screening cloud.

PACS numbers: 78.60.Lc, 78.67.Hc, 78.40.Fy, 72.10.Fk

Introduction.— Exchange interactions between a singly-occupied quantum dot (QD) and a fermionic bath (FB) of itinerant electrons in the bulk lead to the formation of a Kondo state [1–3]. When this many-body ground state is coupled to an optically excited trion state (with an additional QD electron-hole pair, see Fig. 1) by a laser field of vanishingly small Rabi frequency Ω, the resulting emission spectrum at low FB temperatures T is highly asymmetric [4, 5]. Within the energy range defined by Kondo temperature $T_{\rm K} \gg T$, the spectral line shape is characterized by a power-law singularity. The Anderson orthogonality catastrophe determines the corresponding non-integer exponent and ensures that in this limit there is no coherent light scattering. In the opposite limit of large Ω and vanishing exchange interaction ($T_K \to 0$), the emission spectrum consists of a Mollow triplet and an additional δ-function peak [6–8]. While the latter stems from coherent Rayleigh scattering, the Mollow-triplet originates from incoherent transitions between dressed states that are themselves superpositions of the original excited trion and the singly-charged ground states.

In this Letter, we analyze the interplay between strong exchange and non-perturbative laser couplings. By using a combination of numerical and analytical techniques, we find that the emission line-shape in the limit $T \ll \Omega \ll T_K$ is drastically different than either of the two limits discussed above. Our findings demonstrate the emergence of a new quantum-correlated many-body state, which is a coherent superposition of the Kondo and trion states (see Fig. 1). In the Kondo state, the electron spin is screened by a spin cloud in the FB, formed within distance $\propto 1/T_{\rm K}$ from the dot, which is missing in the bare trion state. The new quantum-correlated state is associated with the formation of an additional "secondary" screening cloud at larger distances that compensates for the differences in local occupancies between the Kondo and trion states. Interestingly, the secondary screening process is also of the Kondo universality class. It sets in at the renormalized Rabi frequency Ω^* ("secondary Kondo temperature"), whose power-law dependence, $\Omega^* \propto \Omega^{4/3}$, stems from the primary Kondo correlations. This new energy scale manifests itself in the location of a broad peak in the emission spectrum. The peak's tail exhibits a crossover between two power-law functions corresponding to the primary and secondary Kondo correlations, respectively. We also find that the emergence of the secondary screening cloud coincides with the recovery of the δ-function peak in the emission spectrum, whose weight scales as $\delta_{\rm weight} \propto \Omega^{2/3}$. These predictions should be observable in experiments based on self-assembled QDs with strong tunnel coupling to a degenerate electron gas [5].

Model.— We assume laser light propagating along the heterostructure growth direction with circular polariza-

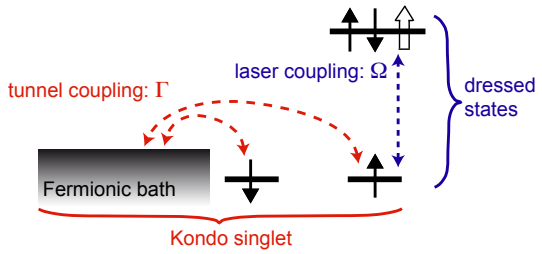

FIG. 1. (Color online) Competition between tunnel coupling and laser coupling on the QD $|\uparrow\rangle$ state. While tunnel coupling would lead to a Kondo singlet state strongly correlated to the FB, a polarized laser creates dressed QD states. The characteristic energy scales in competition are the Kondo temperature $T_{\rm K}$ and the Rabi frequency Ω, respectively.

tion $\sigma_{\rm L}=+1$ and a frequency $\omega_{\rm L}$ close to the QD X^- resonance. We model the system by an excitonic Anderson model [4, 9] augmented by a non-perturbative laser-QD interaction in the rotating wave approximation. We set $\hbar=k_{\rm B}=1$ and assume zero magnetic field. In addition, the optical selection rules imply that when the laser field is right-hand circularly polarized ($\sigma_L=+1$), only the spin-up electron state will be optically excited, leading to the generation of a trion state in which the hole will be in the $\Uparrow$ spin state (Fig. 1). We thus omit the corresponding indices. The spontaneous emission rate $\gamma_{\rm SE}$ is assumed to be negligibly small compared to all other energy scales. In the rotating frame, the Hamiltonian, to be called "Rabi-Kondo model", thus reads:

$$\begin{aligned}H=&\sum_{\sigma}\left(\varepsilon_{\rm e}-U_{\rm eh}n_{\rm h}\right)n_{{\rm e}\sigma}+Un_{{\rm e}\uparrow}n_{{\rm e}\downarrow}+\left(\varepsilon_{\rm h}-\omega_{\rm L}\right)n_{\rm h}\\&+\sum_{k\sigma}\varepsilon_{k\sigma}c^{\dagger}_{k\sigma}c_{k\sigma}+\sqrt{\Gamma/\left(\pi\rho\right)}\sum_{k\sigma}\left(e^{\dagger}_{\sigma}c_{k\sigma}+{\rm H.c.}\right)\\&+\Omega e^{\dagger}_{\downarrow}h^{\dagger}+{\rm H.c.}\end{aligned}\qquad(1)$$

The first three terms define the QD Hamiltonian, where $n_{{\rm e}\sigma}=e^{\dagger}_{\sigma}e_{\sigma}$, $n_{\rm h}=h^{\dagger}h$, while $e^{\dagger}_{\sigma}$ and $h^{\dagger}$ are creation operators for QD spin-σ electrons ($\sigma=\uparrow,\downarrow$ or ±1) and holes, respectively. We denote the spin-degenerate QD electron level energy by $\varepsilon_{\rm e}$, the hole level energy by $\varepsilon_{\rm h}$, and the laser frequency by $\omega_{\rm L}$. We account for intra-dot Coulomb interaction by $U_{\rm eh}>0$ and $U>0$. To ensure a separated low-energy subspace formed by the three states in Fig. 1, the laser detuning from the bare QD transition, $\delta_{\rm L}=\omega_{\rm L}-\varepsilon_{\rm e}-U-\varepsilon_{\rm h}+2U_{\rm eh}$, has to be small in the sense defined below. The first term on the second line of Eq. (1) models a noninteracting conduction band (the FB) with half-bandwidth D_0, symmetric around the Fermi energy $\varepsilon_{\rm F}=0$, and constant density of states $\rho\equiv1/(2D_0)$ per spin. This choice is adequate, since only energies in the vicinity of $\varepsilon_{\rm F}$ are important. The second term on the second line of Eq. (1) is the hybridization term, describing tunneling between FB and QD. We assume $T\ll\Gamma\ll U\simeq U_{\rm eh}\ll D\ll\varepsilon_{\rm h}$, $\omega_{\rm L}$ and investigate a situation where the QD carries one negative charge $\langle n_{{\rm e}\uparrow}+n_{{\rm e}\downarrow}-n_{\rm h}\rangle\simeq1$, [10]. Finally, the QD-laser coupling is described by the last term in Eq. (1); it connects the hole-subspace (defined with projector $P_{\rm h}=n_{\rm h}$) to the subspace without hole ($P_\gamma=1-n_{\rm h}$). In the P_γ-subspace the system is susceptible to Kondo physics; the Kondo temperature $T_{\rm K}$ associated with the projected Hamiltonian $P_\gamma HP_\gamma$ is $T_{\rm K}=\sqrt{\Gamma U/2}\exp\left[-\pi\left|\varepsilon_{\rm e}\left(\varepsilon_{\rm e}+U\right)\right|/\left(2U\Gamma\right)\right]$ [1, 2].

Emission spectrum.— The main physical observable which we will examine throughout this paper is the emission spectrum at detuning ν from the laser frequency $\omega_{\rm L}$. It is proportional to the spectral function

$$S\left(\nu\right)=\sum_{n,m}\varrho_m\left|\langle n|he_{\downarrow}|m\rangle\right|^2\delta\left(E_n-E_m+\nu\right),\qquad(2)$$

where $|m\rangle$ and E_m are eigenstates and eigenenergies of the Rabi-Kondo model. We assume that spontaneous emission has a negligible effect on the system's steady state, which is taken to be a thermal state in the rotating frame at the temperature T of the solid state environment, $\varrho_m=Z^{-1}e^{-E_m/T}$ [9], and concentrate on $T=0$. We denote the energy difference between the Kondo singlet state $|{\rm KS}\rangle$ (ground state of $P_\gamma HP_\gamma$) and the trionic state $|{\rm X}^-\rangle$ without a screening cloud in the FB (ground state of $P_{\rm h}HP_{\rm h}$) by $\Delta E=E_{0,{\rm h}}-E_{0,\gamma}$. To simplify the discussion we will address mostly the $\Delta E=0$ case (achieved by properly adjusting the laser frequency ω_L) below, and defer the treatment of finite ΔE to the Supplemental Material (SM) [9].

Since the total spectral weight is given by $\langle n_{\rm h}n_{{\rm e}\downarrow}\rangle\simeq O\left(\langle n_{\rm h}\rangle\right)$, it is strongly dependent on ΔE and Ω. To enable mutual comparison between results for different values of these parameters we normalize all spectra as $\tilde{S}\left(\nu\right)\equiv S\left(\nu\right)/\langle n_{\rm h}\rangle$. Fig. 2 shows typical Numerical Renormalization Group (NRG) [11–13] results for $\tilde{S}\left(\nu\right)$.

For $\Omega\gg T_{\rm K}$ no signatures of Kondo physics are expected. The emission spectrum can be completely understood in terms of a QD dressed state ladder with the assumption of zero spontaneous emission rate and an intra-manifold, FB-induced decay process [14, 15]. The spectrum has two peaks: a broad peak at $|\nu_{\rm max}|=2\Omega$ and a delta-peak at $\nu=0$, both with equal weight 0.25 [see Figs. 2 (blue line) and 3].

The situation is much more interesting for the Kondo-

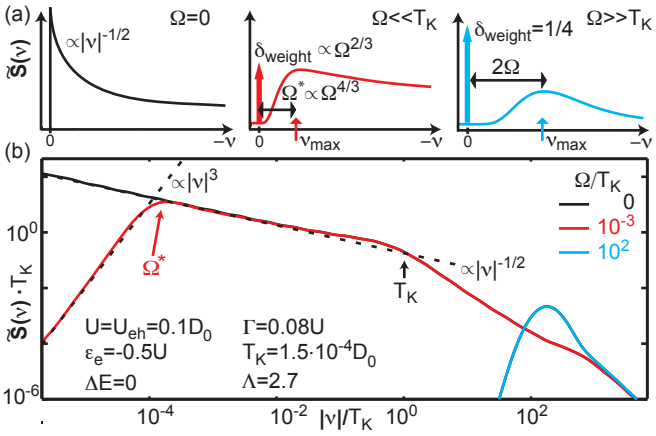

FIG. 2. (Color online) Normalized emission spectra $\tilde{S}\left(\nu\right)$ for $\Delta E=0$ and three characteristic choices for $\Omega/T_{\rm K}$. (a) Schematic plots; thick arrows indicate Dirac δ-peaks. (b) NRG results for the Rabi-Kondo model Eq. (1): Log-log plot of the broad emission peak $[\tilde{S}\left(\nu<0\right)]$. Dirac δ-peaks are omitted here for clarity. Thick solid lines denote spectra, while the straight dashed lines represent power-law asymptotes. See the text for further details. We have confirmed similar results for the non-symmetric case $\varepsilon_{\rm e}\neq-U/2$ and $U\neq U_{\rm eh}$ as long as $\langle n_{{\rm e}\uparrow}+n_{{\rm e}\downarrow}-n_{\rm h}\rangle\simeq1$.

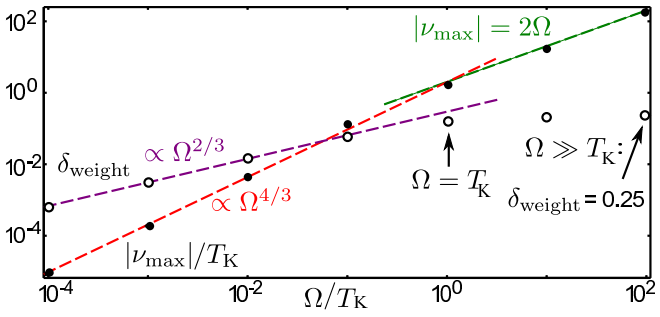

FIG. 3. (Color online) NRG results for the Rabi-Kondo model Eq. (1): Position of broad peak $|\nu_{\max}|$ (dots) in emission spectrum and weight of δ-peak (circles) vs. $\Omega/T_{\rm K}$. Thick dashed lines are power-law fits to Eqs. (6) and (8).

dominated regime, $\Omega \ll T_{\rm K}$, which we consider henceforth. In this regime one might attempt to treat the QD-laser coupling [last term in the Hamiltonian Eq. (1)] as a perturbation. This would yield a spectrum that is essentially the same as the $\Omega = 0$ spectrum calculated in Ref. 4. However, we will show momentarily that this is correct only if the frequency $|\nu|$ is larger than a new energy scale $\Omega^* \ll T_{\rm K}$.

Effective model.— In order to understand this restriction on the perturbative treatment of the QD-laser coupling, as well as to derive the low-frequency behavior, it is useful to introduce an effective Hamiltonian, valid in the entire regime $|\nu| \ll T_{\rm K}$. It can be thought of as the result of integrating out the degrees of freedom in the Rabi-Kondo model H with energies larger than $T_{\rm K}$. For $|\nu| \ll T_{\rm K}$ we can concentrate on just two states of the QD together with these FB high-energy degrees of freedom: The Kondo singlet state $|{\rm KS}\rangle$, featuring a screening cloud stretching a distance $\propto 1/T_{\rm K}$ into the FB, and the trion state $|{\rm X}^-\rangle$, with no screening cloud. We thus replace the QD and the high-energy degrees of freedom of the FB (with energies $\gtrsim T_{\rm K}$) by a two level system (TLS) or a pseudospin, whose $\sigma'_z = \pm 1$ (σ'_i being the Pauli matrices) eigenstates correspond to the trion and Kondo states, respectively. These two states are coupled by the laser light and are split in energy (in the rotating frame) by the laser frequency detuning. Furthermore, the electrons with energies $\lesssim T_{\rm K}$ experience different scattering phase shifts depending on the state of the TLS: in the $|{\rm KS}\rangle$ state the electrons in the FB experience $\delta_\sigma^{\rm KS} = \pi/2$ phase shifts, while in the $|{\rm X}^-\rangle$ state the phase shifts are $\delta_\sigma^{{\rm X}^-} = (1+\sigma)\pi/2$ by the Friedel sum rule [16] (see the discussion of the screening cloud below for further details). All this is captured by the following Hamiltonian:

$$H' = \sum_{k\sigma} \varepsilon'_{k\sigma} c'^\dagger_{k\sigma} c'_{k\sigma} + \Omega' \sigma'_x + \frac{\Delta E'}{2} \sigma'_z + \sigma'_z \sum_{\sigma,k,k'} U'_\sigma c'^\dagger_{k\sigma} c'_{k'\sigma}. \tag{3}$$

The first term is the Hamiltonian of the low-energy part of the original FB, and has the same form as before [cf. Eq. (1)], but with a reduced half bandwidth $D'_0 \sim T_{\rm K}$. The second term in H' describes optical excitations, with $\Omega' = \Omega \langle {\rm KS}|he_\downarrow|{\rm X}^-\rangle_{T_{\rm K}} \propto \Omega$, where the subscript $T_{\rm K}$ denotes taking the matrix elements with states confined to the FB degrees of freedom of energy $\gtrsim T_{\rm K}$. The third term in H' is the detuning, with $\Delta E' = \Delta E$ up to an Ω-dependent shift, as we have also verified numerically. Finally, the last term in H' accounts for the scattering of the FB electrons by the TLS. To mimic the scattering phase shift differences $\delta_\sigma^{\rm KS} - \delta_\sigma^{{\rm X}^-} = -\sigma\pi/2$ of the FB electrons in the two states of the TLS, we take $\tan^{-1}(\pi\rho' U'_\sigma) = -\sigma\pi/4$, [9]. For $|\nu| < T_{\rm K}$, the emission spectrum $\tilde{S}(\nu)$ for the Rabi-Kondo model is reproduced qualitatively by $\tilde{S}'(\nu)$ computed as in Eq. (2), but with H' and σ'_- taking the place of H and $he_\downarrow$, respectively [9].

Intermediate-frequency behavior and the emergence of a new energy scale.— To lowest order in Ω', the behavior of $\tilde{S}'(\nu)$ is governed by the Anderson orthogonality between the TLS states $|{\rm KS}\rangle$ and $|{\rm X}^-\rangle$, caused by the difference in phase shifts the FB electrons experience in the two states. The spectrum thus behaves as a power law, $\tilde{S}'(\nu) \sim |\nu|^{2\eta'_x - 1}$, with

$$2\eta'_x = \left(\frac{\delta_\uparrow^{\rm KS} - \delta_\uparrow^{{\rm X}^-}}{\pi}\right)^2 + \left(\frac{\delta_\downarrow^{\rm KS} - \delta_\downarrow^{{\rm X}^-}}{\pi}\right)^2 = \frac{1}{2} \tag{4}$$

being the Anderson orthogonality exponent [13, 17], in agreement with the $\Omega = 0$ results of Ref. 4. This implies that the hybridization operator σ'_x has a scaling dimension $\eta'_x = 1/4 < 1$ and is thus a relevant perturbation near the fixed-point $\Omega' = 0$. In other words, the leading-order renormalization group (RG) flow equation for Ω' as one decreases the cutoff D' from its bare value D'_0 is [18]

$$D' \frac{{\rm d}}{{\rm d}D'} \left(\frac{\Omega'}{D'}\right) = (\eta'_x - 1) \frac{\Omega'}{D'}. \tag{5}$$

The dimensionless coupling Ω'/D' therefore grows and becomes of order one when the cutoff reaches the scale

$$\Omega^* = D'_0 \left(\frac{\Omega'}{D'_0}\right)^{1/(1-\eta'_x)} \sim T_K \left(\frac{\Omega}{T_K}\right)^{4/3} \ll T_K. \tag{6}$$

Hence, one may treat the term $\Omega'\sigma'_x$ [corresponding to the last term in Eq. (1)] as a perturbation only if $|\nu| \gg \Omega^*$. The power-law $\tilde{S}(\nu) \sim |\nu|^{-1/2}$ thus applies at intermediate frequencies, $\Omega^* \ll |\nu| \ll T_{\rm K}$. The power-law divergence of the spectrum is cut off around $|\nu| \sim \Omega^*$ [13], resulting in a maximum in the spectrum at this scale, as confirmed by the NRG data shown in Figs. 2 and 3. The emergence of this new energy scale is one of our central results. At low frequencies, $|\nu| \ll \Omega^*$, the physics is governed by a new fixed point, which we now discuss.

Secondary Kondo screening.— To understand this new fixed point we recall that since H' describes a TLS coupled to an Ohmic reservoir, it belongs to the same universality class as the anisotropic Kondo model. This "secondary", or auxiliary, Kondo model should not be confused with the original "primary" isotropic Kondo model for the QD spin. The role of the secondary Kondo temperature is played by Ω^*. Thus, at energies smaller than Ω^*, the original system flows to a strong-coupling fixed point featuring a strong hybridization between the Kondo and trion sectors, as confirmed by the NRG level-flow data [9]. The low-energy behavior is universal when energies are measured in units of Ω^*.

One of the predictions of this "secondary Kondo" picture is that the ground state of H for $\Omega \ll T_K$ and $\Delta E = 0$ is an equal-amplitude superposition of the Kondo and trion states, with some secondary screening cloud, whose distance from the QD is larger than the Kondo length $\propto 1/T_{\rm K}$ associated with the primary screening cloud. To understand this nested screening cloud structure, consider a reference state where the QD valence levels are filled and its conduction levels are empty. In the state $|{\rm KS}\rangle$ (ground state for $\Omega = 0$, $\Delta E > 0$) the average electronic population is shifted with respect to the reference state by 1/2 electron per spin direction and the total spin is zero, corresponding to the aforementioned phase shifts $\delta_\sigma^{\rm KS} = \pi/2$ by the Friedel sum rule [16]. Thus, the correlation function between the dot spin and the total reservoir spin is $\left\langle S^z_{\rm QD} S^z_{\rm FB}\right\rangle = -1/4$. This implies that when projecting into the subspace with spin up (down) in the dot, the reservoir has a net additional single spin down (up) electron [19] within a screening cloud up to a distance $\propto 1/T_{\rm K}$ from the QD. If, on the other hand, $\Omega = 0$ but $\Delta E < 0$, the system is in the trion state $|{\rm X}^-\rangle$ with two electrons and a spin-up hole; overall, only the spin-up population is shifted (by 1) with respect to the reference state, leading to $\delta_\sigma^{\rm X^-} = (1+\sigma)\pi/2$, as mentioned above. Turning on the laser source Ω, when $\Delta E = 0$ the ground state is an equal-amplitudes superposition (of spatially restricted versions) of the Kondo and trion states ($\langle P_{\rm h}\rangle = \langle P_\gamma\rangle = 1/2$) as depicted in Fig. 4(c). In analogy with the screening of a QD spin in a Kondo singlet, the FB screens the different spin configurations of the $|{\rm X}^-\rangle$ and $|{\rm KS}\rangle$ states, adding half an electron spin up to the Kondo state and half a spin down to the trion state within distance $\sim 1/\Omega^*$ of the QD [20]. This nested screening cloud indeed appears in the NRG results as seen in Fig. 4, further confirming our effective low-energy description.

Low-frequency behavior and δ-peak.— To derive the low-frequency behavior of the spectrum, as well as the appearance and weight of the elastic δ-peak mentioned in the introduction, we need to make the notion of "secondary Kondo effect" more precise. This can be done formally by transforming H' into a secondary Kondo model in two stages: (i) Upon bosonization of the FB [21] H' becomes the spin-boson model with Ohmic dissipation [22]; (ii) the spin-boson model can be mapped onto the anisotropic Kondo model [1, 2]:

$$H'_{\rm K} = -iv_F \sum_{\sigma=\uparrow,\downarrow} \int {\rm d}x \psi^\dagger_\sigma(x)\partial_x\psi_\sigma(x) + \frac{J_z}{2} S'_z s'_z(0) + \frac{J_{xy}}{2} S'_- s'_+(0) + {\rm H.c.} - \Delta E_z S'_z, \quad (7)$$

where $v_F = 1/(\pi\rho)$ is the Fermi velocity, S'_i are the components of the auxiliary Kondo impurity spin, and $s'_i(0) = \sum_{\sigma,\sigma'} \psi_\sigma(0)^\dagger \tau_i^{\sigma\sigma'} \psi_{\sigma'}(0)/2$ (τ_i being the Pauli matrices) are the FB spin density components in the vicinity of the impurity. Under this mapping $\sigma'_z = 2S'_z$ (hence $\Delta E_z \propto \Delta E'$) but $\sigma'_+ \to S'_+ s'_-(0)$.

One can now use known results on H'_K to find the low-frequency ($|\nu| \ll \Omega^*$) behavior of the emission spectrum of H'. By the above mapping $\tilde{S}'(\nu)$ is proportional to the spectral function of the retarded correlator of $S'_+ s'_-(0)$ with its conjugate in H'_K. Since the anisotropic antiferromagnetic Kondo problem flows to the same strong-coupling fixed point as the isotropic version, the calculation of low-frequency power-law exponents can be done in the isotropic case $J_z = J_{xy}$, where the correlation function of $S'_+ s'_-(0)$ can be replaced by the $S'_z s'_z(0)$ correlation function. At low energies, after the impurity spin is screened by the FB, $S'_z s'_z(0)$ can be replaced by the square of the local density of the z-component of the electronic spin, which is a four-fermion operator. Thus, in the absence of an effective magnetic field, $\Delta E_z = 0$, its correlation function scales at long times ($t > 1/\Omega^*$) as t^{-4}, leading to a $\sim |\nu|^3$ low-frequency behavior of the corresponding spectral function. The same then applies to $\tilde{S}^{(\prime)}(\nu)$ in the regime $|\nu| \ll \Omega^*$. This is indeed the behavior of the NRG results, cf. Fig. 2 and SM [9].

The above picture leads to another implication for the spectrum: Since the relevant perturbation $\Omega'\sigma'_x$ strongly-hybridizes, and thus cuts off the Anderson orthogonality between the $|{\rm KS}\rangle$ and $\left|{\rm X}^-\right\rangle$ states at energy scales smaller than Ω^* [13], a Dirac δ-peak is now allowed to appear in the spectrum. By the definition of $S'(\nu)$, the weight of the delta-peak is $\delta_{\rm weight} = |\langle\sigma'_x\rangle|^2$. Since Ω^* is the only low-energy scale, we expect that $\Omega' \langle\sigma'_x\rangle \propto \Omega^* \propto \Omega'^{4/3}$. Hence, $\langle\sigma'_x\rangle \propto \Omega'^{1/3} \propto \Omega^{1/3}$, leading to

$$\delta_{\rm weight} \propto \Omega^{2/3}, \quad (8)$$

which is in excellent agreement with the NRG results, Fig. 3 [23].

Conclusions.— Laser excitation of a quantum dot in the Kondo regime can lead to a new correlated state at energies below a renormalized Rabi frequency Ω^* [Eq. (6)]. The Rabi coupling occurs between a many-body Kondo state and a trion state and is accompanied by formation of an unusual secondary spin-screening cloud in the FB (Fig. 4). The new correlated state gives

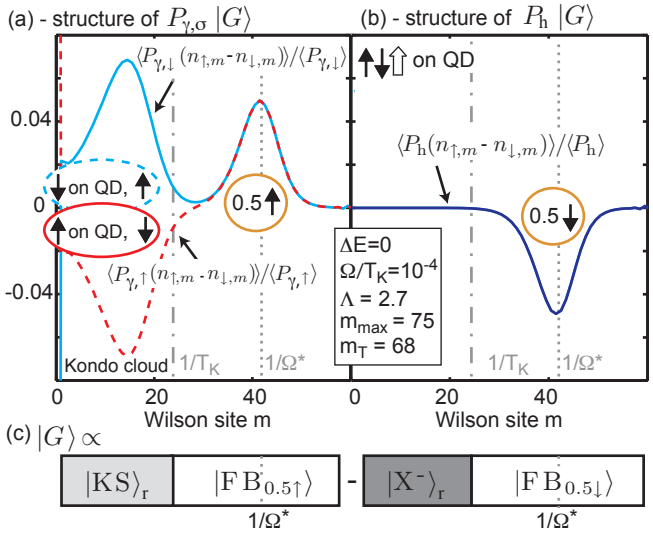

FIG. 4. (Color online) NRG results for the Rabi-Kondo model Eq. (1): Distribution of magnetization $n_{\uparrow,m} - n_{\downarrow,m}$ along the Wilson chain, obtained after acting with QD projectors (a) $P_{\gamma,\sigma} = P_\gamma n_{e,\sigma}(1 - n_{e,\bar{\sigma}})$ and (b) P_h on the ground state $|G\rangle$, for $\Omega/T_K = 10^{-4}$ and $\Delta E = 0$ at $T = 2 \cdot 10^{-14} D_0$ (corresponding to the energy scale of Wilson site $m_T = 68$). Even-odd oscillations have been averaged out. The QD is represented by site zero. In (a), the Kondo state, restricted to a region of size $\lesssim 1/T_K$ (subscript r), approximately $|KS\rangle_r \propto |\uparrow\rangle|FB_\downarrow\rangle_r - |\downarrow\rangle|FB_\uparrow\rangle_r$, features a singlet configuration with FB magnetization opposite to that of the QD (left dip/peak structure). In (b) the $|X^-\rangle_r$ trivial FB configuration appears within the same length scale. The presence of a laser ($\Omega > 0$) combines the states $|KS\rangle_r$ and $|X^-\rangle_r$ into a new ground state $|G\rangle \propto |KS\rangle_r |FB_{0.5\uparrow}\rangle - |X^-\rangle_r |FB_{0.5\downarrow}\rangle$, where FB states $|FB_{0.5\sigma}\rangle$ carry a magnetization of half a spin σ at distance $1/\Omega^*$ [peak in (a)/ dip in (b)]. The spin orientation of the secondary screening cloud is controlled by the laser polarization $\sigma_L = +1$. (c) Schematic drawing of nested screening clouds in the ground state.

rise to a specific line shape of the resonance fluorescence spectrum. It is characterized by two peaks (Figs. 2 and 3): (i) A broad peak centered around $|\nu| = \Omega^*$, with an inverse-square root high-frequency tail [Eq. (4)], resulting from the Anderson orthogonality between ground and post-emission states resembling $|X^-\rangle$ and $|KS\rangle$ at length scales $\ll 1/\Omega^*$. A Fermi-liquid type low-frequency tail stems from the cut-off of the orthogonality by the relevant Rabi coupling, as ground and post-emission state share a "common" FB configuration at length scales $\gg 1/\Omega^*$ due to the secondary screening cloud. (ii) This common FB region leads to a Dirac δ-peak at $\nu = 0$, whose weight scales as a power-law with the Rabi frequency Ω [Eq. (8)]. The Ω dependence of the strength of coherent Rayleigh scattering in the presence of a finite spontaneous emission rate γ_{SE} remains an open question.

Acknowledgements.— We acknowledge helpful discussions with A. Rosch. This work was supported by an ERC Advanced Investigator Grant (B.S. & A.I.). H.E.T. acknowledges support from the Swiss NSF under Grant No. PP00P2-123519/1. M.G. is supported by the Simons Foundation and the BIKURA (FIRST) program of the Israel Science Foundation, L.I.G. by NSF DMR Grant No. 1206612, J.v.D., M.H. and A.W. by the DFG via NIM, SFB631, SFB-TR12, and WE4819/1-1.

[1] A. Hewson, *The Kondo Problem to Heavy Fermions* (Cambridge University Press, Cambridge, 1993).
[2] D. L. Cox and A. Zawadovski, Adv. Phys. **47**, 599 (1998).
[3] L. Kouwenhoven and L. Glazman, Physics World **14**, 33 (2001).
[4] H. E. Türeci *et al.*, *Phys. Rev. Lett.* **106**, 107402 (2011).
[5] C. Latta *et al.*, Nature (London) **474**, 627 (2011).
[6] B. R. Mollow, Phys. Rev. **188**, 1969 (1969).
[7] E. Flagg *et al.*, Nature Phys. **5**, 203 (2009).
[8] C. Matthiesen, A. N. Vamivakas, and M. Atatüre, Phys. Rev. Lett. **108**, 093602 (2012).
[9] See Supplemental Material.
[10] This requires $\Gamma \ll -\varepsilon_e, \varepsilon_e + U, -(2\varepsilon_e - 2U_{eh} + U), -\varepsilon_e + U_{eh} - U$.
[11] R. Bulla, T. A. Costi, and T. Pruschke, Rev. Mod. Phys. **80**, 395 (2008).
[12] A. Weichselbaum and J. von Delft, Phys. Rev. Lett.**99**, 076402 (2007); A. Weichselbaum, arXiv:1209.2062.
[13] W. Münder, A. Weichselbaum, M. Goldstein, Y. Gefen, and J. von Delft, Phys. Rev. B **85**, 235104 (2012).
[14] B. Sbierski and A. Imamoglu. (to be published).
[15] In the more realistic situation of a finite rate γ_{SE}, a Mollow *trip*let with a broadened peak at $\nu = 0$ and a blue detuned peak at $\nu = 2\Omega$ may develop.
[16] J. Friedel, Phil. Mag. **43**, 153 (1952); Can. J. Phys. **34**, 1190 (1956); D. C. Langreth, Phys. Rev. **150**, 516 (1966).
[17] B. Roulet, J. Gavoret, and P. Nozières, Phys. Rev. **178**, 1072 (1969); P. Nozières, J. Gavoret, and B. Roulet, *ibid.* **178**, 1084 (1969); P. Nozières and C. T. De Dominicis, *ibid.* **178**, 1097 (1969).
[18] J. Cardy, Scaling and Renormalization in Statistical Physics (Cambridge University Press, Cambridge, 1996).
[19] I. Affleck, arXiv:0911.2209.
[20] The total electron number is of course integer; if the screening cloud contains fractions of electrons, the rest is spread over the entire system, and thus does not contribute to the charge and spin distributions in the thermodynamic limit.
[21] A. Gogolin, A. A. Nersesyan, and A. M. Tsvelik, *Bosonization and Strongly Correlated Systems* (Cambridge University Press, Cambridge, 1998).
[22] U. Weiss, *Quantum Dissipative Systems* (World Scientific, Singapore, 1999).
[23] However, further work including spontaneous emission in the theoretical treatment would have to revisit the actual form of the spectrum for $|\nu| < \gamma_{SE}$ and the distribution of δ_{weight} into an elastic and inelastic contribution.